Arabian Journal of Chemistry (2020) 13, 8481–8488

King Saud University

Arabian Journal of Chemistry

www.ksu.edu.sa
www.sciencedirect.com

ORIGINAL ARTICLE

Photocatalytic degradation of deltamethrin by using Cu/TiO_2/bentonite composite

Sana Ahmad *, **Amina Yasin**

Department of Chemistry, Lahore College for Women University, Lahore, Pakistan

Received 17 January 2020; accepted 25 July 2020
Available online 5 August 2020

KEYWORDS

Bentonite;
Titania;
Composite;
Deltamethrin;
Photodegradation

Abstract In the present work, titanium dioxide nanoparticles and Cu/TiO_2/bentonite composites were prepared by using thermal decomposition and reduction method. The samples were characterized by FTIR, XRD, TGA and SEM. The photocatalytic properties of the prepared composites were studied for the degradation of deltamethrin. Several factors on degradation process were investigated such as total time of light irradiation, pH of the solution and concentration of catalyst to optimize the reaction conditions. It was observed that the prepared metal doped composite possesses high efficiency for the degradation of the insecticide. The degradation process follows first order kinetics. Antibacterial activity of the synthesized composites was also studied and the result shows that obtained composites possess good antibacterial activity.

1. Introduction

One of the greatest concerns of mankind is to control and prevent environmental contamination. Advanced techniques that can diminish or eliminate pollution need to be developed. Photo degradation of harmful contaminants is one such technique that can be successfully utilized. Nanostructural materials have recently become a center of attention due to their tremendous biological and pharmaceutical applications and interesting properties (Barbosa et al., 2015; Tamayo et al., 2016; Samavati and Ismail, 2017). These materials are different from bulk materials and isolated molecules because of their unique optical, electronic and chemical properties (Radhakrishnan and Beena, 2014). Titanium dioxide (TiO_2) as a semiconductor photocatalyst has been successfully utilized for the degradation of different toxins owing to its high photocatalytic activity and mechanical strength (Yu et al., 2015; Li et al., 2016). TiO_2 is an n-type semiconductor and the most widely recognized crystalline forms of TiO_2 are brookite, rutile, and anatase. Anatase has a higher photocatalytic activity than other forms, and therefore is most widely used (Katerina et al., 2014).

TiO_2 shows high photocatalytic activity under UV irradiation due to its wide band gap (3.0–3.2ev) and utilizes a small fraction of solar spectrum which hampers its large scale industrial applications (Daniel et al., 2007; Kim et al., 2015; Islam et al., 2016; Zoltan et al., 2016). The antibacterial activity of TiO_2 is due to the ability to activate free hydroxyl radicals (—OH) by TiO_2 particles. Coinage or noble metal nanoparticles (Ag, Au, Pt, Pd, and Cu) are generally loaded on TiO_2

* Corresponding author.
E-mail address: sana.ahmed@lcwu.edu.pk (S. Ahmad).
Peer review under responsibility of King Saud University.

Production and hosting by Elsevier

https://doi.org/10.1016/j.arabjc.2020.07.019
1878-5352

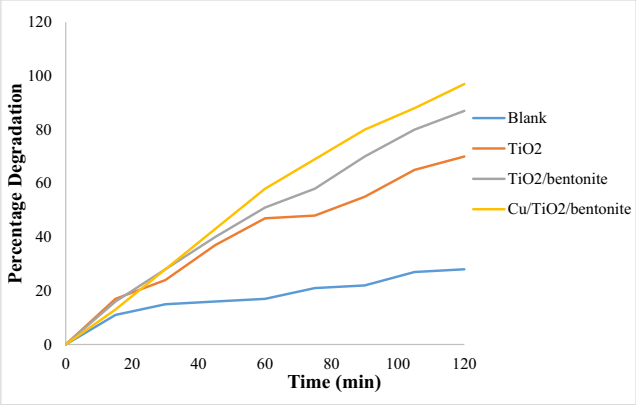

Graph 1 Effect of time on percentage degradation.

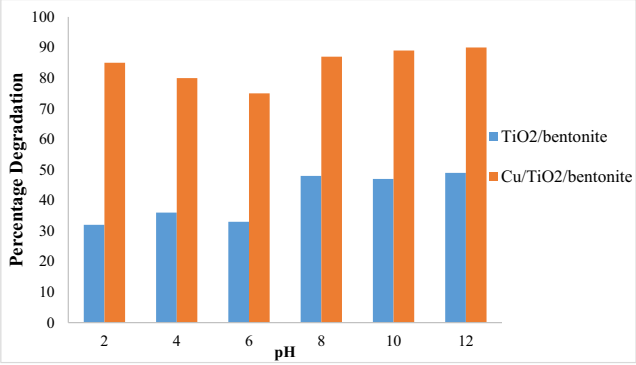

Graph 2 pH effect on percentage degradation.

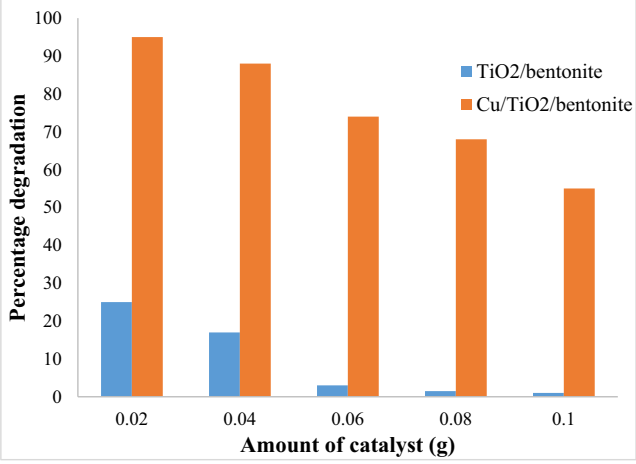

Graph 3 Effect of concentration on percentage degradation.

to make it visibly active. Copper ions have demonstrated antimicrobial activity against a wide range of microorganisms, such as Staphylococcus aureus, Salmonella enteric, Escherichia coli, etc. The metal nanoparticles play an active role in electron transfer process and enhance the photocatalytic efficiency (Daghrir et al., 2013; Valisaki et al., 2015; Qi et al., 2014; Fu and CaO, 2015; Jesus et al., 2017).

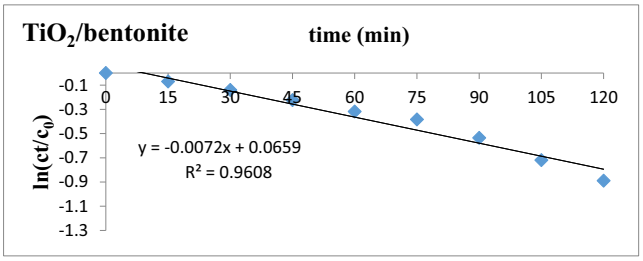

Graph 4 Kinetics of degradation of Deltamethrin in the presence of TiO_2/bentonite composite $t_{0.5}$ = **0.693/0.0072 = 96 min.**

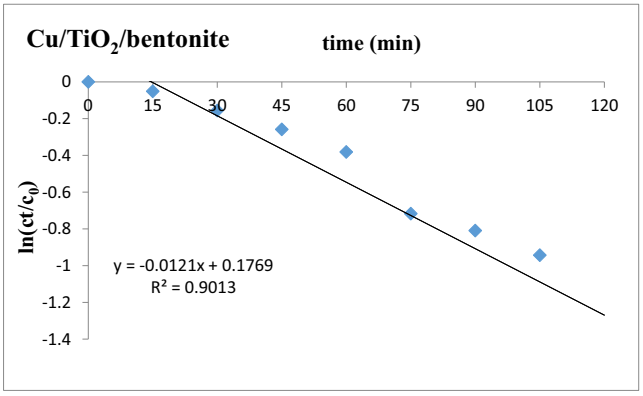

Graph 5 Kinetics of degradation of Deltamethrin in the presence of Cu/TiO_2/bentonite composite $t_{0.5}$ = **0.693/0.0121 = 43 min.**

High surface area of the catalyst is crucial to achieve high activity. However, TiO_2 nanoparticles have a tendency to agglomerate and make large sized particles with low surface area. Therefore, most studies dealing with photocatalyst based on TiO_2 particle have chosen to disperse them throughout matrices such as silica, alumina, clays in order to increase the number of surface-active sites and to improve the interaction with the pollutant (Chien-Wei and Chechia, 2020; Hsiao-Han et al., 2019).

Clays can be used as a support for the metal loaded TiO_2, as they are able to adsorb organic substance on their external surfaces as well as within their interlamellar spaces and hence increase the overall removal of the pollutant (Amit et al., 2017). Bentonite is commonly used due to its easy availability and its presence improves the mechanical properties of the composites (Rashid et al., 2016; Szczepanik, 2017; Papoulis et al., 2019; Seftel et al., 2015).

In this paper, thermal decomposition method was used to prepare copper doped and undoped bentonite supported TiO_2 composites. The prepared Cu/TiO_2/bentonite composite would have good dispersion of copper and TiO_2 nanoparticles on the surface of clay and hence propose better photocatalytic activity and antimicrobial activity. The aim of this work was to investigate the photocatalytic ability of the Cu doped TiO_2/bentonite and undoped TiO_2/bentonite composites for the degradation of pesticides. Based on the above goals, TGA, XRD, FT-IR and SEM were employed to investigate the thermal stability, composition, configuration and morphology of the photocatalysts. The photocatalytic activity of the prepared

materials was investigated for the degradation of deltamethrin taken as a model pesticide.

2. Experimental procedures

2.1. Photocatalyst preparations

Bentonite clay was purchased from BDH, titanium butoxide from Sigma Aldrich, $CuSO_4 \cdot 5H_2O$ from RDH and polyethylene glycol was purchased from Merck. Deltamethrin was purchased from local market.

- Sodium bentonite

Bentonite clay was converted into Na-bentonite by suspending 6 g of bentonite into 0.1 M sodium hydroxide solution. The mixture was stirred for 15 min; the suspension was centrifuged for 10 min at 2500 rpm. The obtained residue was then rinsed with distilled water, and then dried at 110 °C for 12 h.

- Copper nanoparticles

Copper nanoparticles were synthesized through chemical reduction method. Copper (II) sulphate pentahydrate was dissolved in the distilled water. An aqueous solution of polyethylene glycol was added to the solution with vigorously stirring. In the next step, ascorbic acid and sodium hydroxide were dissolved in water and added to the prepared solution. In this step color changed from white to yellow. In the last step, solution of sodium borohydrate was prepared in distilled water and added to the above solution under continuous stirring. An instant color change occurred in the aqueous phase from yellow to reddish black. The appearance of this dark color indicates that reduction reaction had started.

- Titanium dioxide nanoparticles

100 mL butanol was taken and its pH was adjusted to 3 by mixing hydrochloric acid. 1 g titanium butoxide was dissolved in butanol. Obtained solution was stirred for 30 min. After that 80 mL distilled water was added and further stirred for 1 h at room temperature. Gel was obtained and dried at 115 °C for 4 h and then calcined at 400 °C to give a white powder.

- TiO_2/bentonite composite

0.05 g titanium butoxide was added to 50 mL butanol at pH 3. Obtained solution was stirred for 30 min and a suspension of 1.2 g Na-bentonite in 50 mL distilled water was added with vigorous shaking. The resulting solution was stirred for 2 h at room temperature and then centrifuged at 4000 rpm for 10 min. The final product was washed with distilled water and ethanol. The solid product was dried at 115 °C for 4 h and then calcined at 500 °C for 3 h.

- Cu/TiO_2/bentonite composite

A 0.1 M titanium butoxide solution was prepared in butanol and stirred for 30 min. 1.2 g Na-bentonite clay was dispersed into distilled water under continuous stirring until a suspension was formed. Then 0.025 M copper (II) nitrate was dissolved into the titanium butoxide solution followed by the addition of suspension. The suspension was vigorously stirred for 2 h at room temperature and was centrifuged at 4000 rpm for 10 min. The final product was washed with distilled water and ethanol. The solid product was dried at 115 °C for 2 h and then calcined at 400 °C for 3 h.

2.2. Characterization of the samples

The crystal structure of the samples was characterized by powder XRD, employed a scanning rate of 0.04 increment/step in a 2θ ranging from 10 to 80 with Cu Kα radiation and operated at 40 kV and current of 40 mA using D8-Discover X-ray diffractometer. FTIR of the photocatalysts were recorded by using IR tracer-100 SHIMADZU at room temperature in the region of 400–4000 cm^{-1}. The morphology and microstructure of the photocatalysts were examined by HR-SEM from EVOLS-10 instrument operated at an accelerating voltage of 20 kV. The thermal stability of photocatalyst were determined by a SBTQ-600 thermal gravimetric analyzer.

2.3. Photocatalytic degradation

The photocatalytic efficiencies of TiO_2/bentonite composite and Cu/TiO_2/bentonite composite were studied for the degradation of Deltamethrin insecticide under natural sunlight.

2.4. Antibacterial assessment

The antibacterial activities of the samples were evaluated by the well diffusion method. Lyophilized bacteria were reconstituted in nutrient broth and cultured overnight at 37 °C. The bacteria were grown in a nutrient broth medium at 37 °C for 24 h. Wells were formed with the help of sterilized 8 mm cork borer. 50 µl of samples were applied into the wells. Ciprofloxacin was used as a positive control. The plates were placed in the incubator for almost 24–48 h. The diameter of inhibitory zones was measured in mm.

3. Results and discussion

3.1. XRD

The XRD patterns of the Na-bent, Cu nanoparticles, TiO_2 nanoparticles, TiO_2/bentonite composite, and Cu/TiO_2/bentonite composite are shown in Fig. 1. In Fig. 1 b, the peaks located at 19.87°, 21.55°, 27.92°, 28.41°, and 36.31° can be assigned to the Na-bentonite (Zhirong et al., 2011; Erin et al., 2010). Fig. 1 d shows the diffraction peaks located at 36.39°, 43.04°, 50.04°, and 73.49° that can be assigned to Cu nanoparticles (Radhakrishnan and Beena, 2014). The peaks located at 25.7°, 38.41°, 48.01°, 53.84°, 55.03°, and 64.31° shows the diffractions of the anatase phase of TiO_2 (Fig. 1 a) (Desai and Kowshik, 2009). After modification, the noise peaks appeared in Fig. 1 c and 1 e is due to the semi-crystallinity of TiO_2/bentonite composite and Cu/TiO_2/bentonite composite. In Fig. 1 c the diffraction angles of 19.8°, 21.5°,25.7, 26.6°, 28.2, 36.02, 38.41°, 42.82°, 55.03 and 64.31°

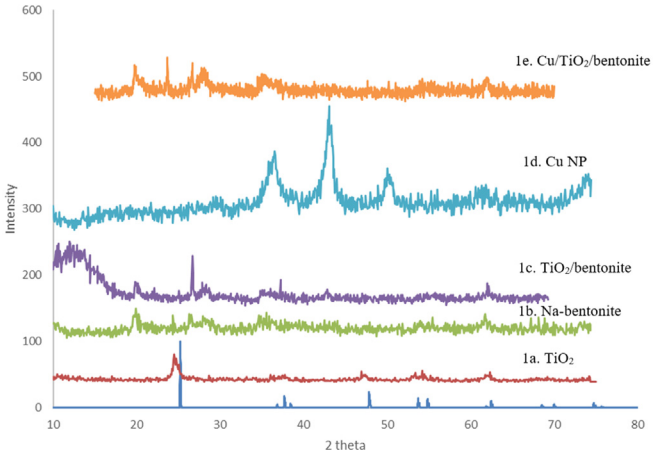

Fig. 1 X-ray diffraction pattern.

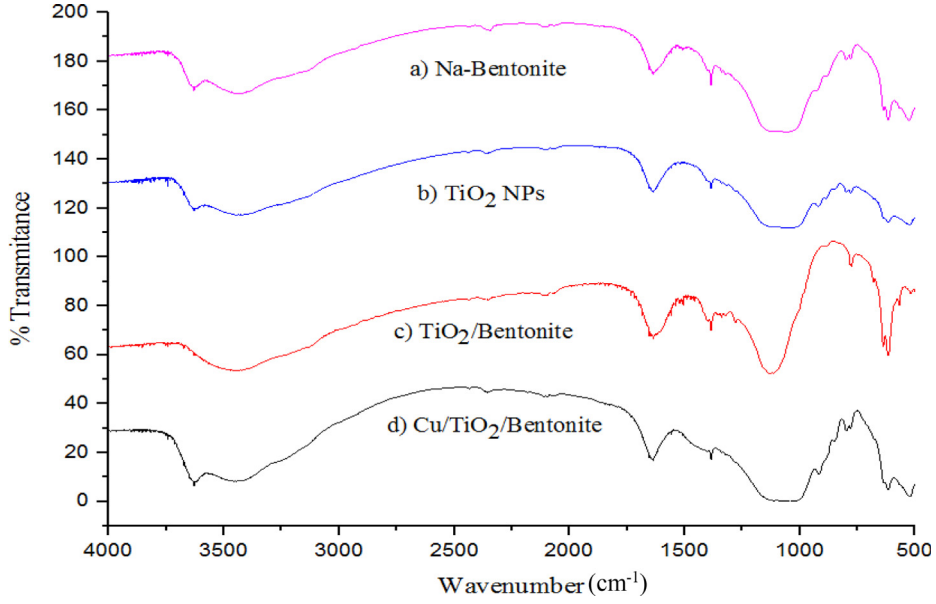

Fig. 2 FTIR spectrum.

shows the TiO_2/bentonite composite. The reflections clearly reflect that TiO_2 nanoparticles have been successfully incorporated in bentonite layered structure. In Fig. 1e the peaks at 19.87°, 21.55°, 25.7°, 28.41°, 36.3°, 38.41°, 43.04°, 55.03, and 62.07 shows the diffraction angles of Cu/TiO_2/bentonite composite. The presence of characteristic peaks of anatase, Cu nanoparticles and bentonite were observed that confirms the formation of our required Cu/TiO_2/bentonite composite.

3.2. FTIR

The FTIR spectra of the samples are given in Fig. 2. In Fig. 2a, two absorption bands at 3629 cm^{-1} and 1635 cm^{-1} corresponds to the stretching and bending vibrations of OH groups in Na-bentonite. A broad band at 3425 cm^{-1} can be assigned to the hydroxyl groups bonded via hydrogen bonds. A sharp band at 796 cm^{-1} indicates quartz mixture in the sample. The band at 686 cm^{-1} is due to the deformation and bending modes of Si—O bonds. The bands at 540 cm^{-1} and 460 cm^{-1} are due to Al—O—Si and Si—O—Si bending vibrations respectively. The band corresponding to Al—Al—OH is observed at 916 cm^{-1}. A very strong absorption band at 1041 cm^{-1} is due to Si—O bending vibration. The bands at 1385 cm^{-1} and 717 cm^{-1} are due to aliphatic hydrocarbons in the Na-bentonite (Zhirong et al., 2011; Desai and Kowshik, 2009).

In Fig. 2b the broadest band observed at 3500 cm^{-1} corresponds to the stretching vibration of hydroxyl group of the TiO_2-NPs. The band observed around 1628 cm^{-1} corresponds to bending modes of Ti—OH. A small peak at 1384 cm^{-1} is related to Ti—O vibration. The bands in the range of 800–400 cm^{-1} correspond to the stretching vibrations of Ti—O

and Ti—O—Ti bonds (Andrea Leon et al., 2017). in Fig. 2c, the absorption peaks between 515 cm^{-1} and 623 cm^{-1} indicates the formation of copper nanoparticles. A sharp peak at 614 cm^{-1} is a characteristic peak for Cu(II)-O bond. The absorption peak at 1620 cm^{-1} and a broad peak observed at 3500 cm^{-1} correspond to the bending and stretching vibration of adsorbed water molecules respectively (Radhakrishnan and Beena, 2014).

In Fig. 2d, a sharp peak at 796 cm^{-1} indicates the presence of quartz mixture in the sample. The bands at 540 cm^{-1} and 460 cm^{-1} are due to Al—O—Si and Si—O—Si bending vibrations respectively. The band corresponding to Al—Al—OH is observed at 916 cm^{-1}. The band at 1635 cm^{-1} corresponds to the bending vibration of H—O groups in water. The band at 618 cm^{-1} is due to the deformation and bending modes of Si—O bonds. The bands at 1384 cm^{-1} and 798 cm^{-1} are due to aliphatic hydrocarbons in the Na-bentonite. The broadest band observed at 3500 cm^{-1} corresponds to the stretching vibration of hydroxyl group in bentonite and on TiO_2 nanoparticles.

In Fig. 2e, the absorption bands observed at 1653 cm^{-1} and at around 3480 cm^{-1} correspond to the stretching frequencies of hydroxyl groups present on the surface of the sample. The bands at 1384 cm^{-1} and 798 cm^{-1} are due to aliphatic hydrocarbons in the Na-bentonite. The broadest band observed at 3500 cm^{-1} corresponds to the stretching vibration of hydroxyl groups. The composite Cu/TiO_2/bentonite mostly exhibited the peaks corresponding to bentonite as bentonite is present in large excess and band related to TiO_2 nanoparticles (between 800 and 400 cm^{-1}) is overlapped by bands corresponding to bentonite.

3.3. SEM

Figs. 3 shows the SEM images of TiO_2/bentonite composite and Cu/TiO_2/bentonite composite. Fig. 3a clearly demonstrate the morphology of the TiO_2/bentonite composite in which TiO_2 nanoparticles are randomly oriented onto the sodium bentonite clay. Large clusters of bentonite clay can be seen with small particles of TiO_2 deposited on their surface. Particles shape was irregular with a particle size ranging from 1 to 20 μm. Fig. 3b shows the randomly oriented Cu and TiO_2 nanoparticles on bentonite clay surface. Particle size ranges from 100 nm to 1 μm for the deposited TiO_2 particles (Nien et al., 2011; Deak et al., 2015; Rosario et al., 2009).

3.4. TGA

Thermal stability of TiO_2/bentonite composite and Cu/TiO_2/bentonite composite was studied with thermogravimetric analysis and the graphs are given in Fig. 4 (a and b). In Fig. 4a, the major weight loss (4%) was observed in the temperature range between 100 and 150 °C due to the evaporation of solvent molecules. A slight weight loss (2%) was observed in the temperature range of 600–750 °C due to the decomposition of bentonite clay. In Fig. 4b, the major weight loss (2%) was observed at the temperature range between 50 and 100 °C due to the evaporation of solvent molecules. The gradual weight loss (2%) was observed at temperature 550–700 °C due to the decomposition of bentonite clay (see Fig. 5)

TGA results clearly indicate that the sample is thermally stable up to 1000 °C. No weight loss was observed after 800 °C owing to high thermal stability of the composite.

4. Photocatalytic activity of composites

4.1. Time effect on degradation

The photocatalytic efficiency of TiO_2/bentonite composite and Cu/TiO_2/bentonite composite was studied at different time intervals. A major difference was found in the photocatalytic degradation efficiency of TiO_2/bentonite composite and Cu/TiO_2/bentonite composite.

The percentage efficiency of degradation was calculated by using the following formula:

$$\text{Percentage Degradation} = [A_0 - A_t/A_0] \times 100$$

Maximum degradation was achieved by using Cu/TiO_2/bentonite composite after 120 min. (See Graph 1)

The results show that the percentage degradation increased dramatically when TiO_2/bentonite composite was used with respect to blank solution. Further increase in the percentage degradation was achieved when Cu/TiO_2 bentonite composite was used that reflects the efficiency of Cu to enhance the catalytic properties of TiO_2. Hence it can be concluded that both the prepared composites are good catalyst for photodegradation of deltamethrin. Up to 97% degradation was observed with Cu/TiO_2/bentonite composite in comparison to 87% and 28% degradation achieved with TiO_2 /bentonite and blank solution respectively.

4.2. Effect of pH on degradation

The photocatalytic degradation efficiency of TiO_2/bentonite composite and Cu/TiO_2/bentonite composite were studied at different pH. The major difference was found in the photocatalytic degradation efficiency of TiO_2/bentonite composite and Cu/TiO_2/bentonite composite. Maximum degradation was observed at pH 12 for both TiO_2/bentonite and Cu/TiO_2/bentonite composite as shown in Graph 2.

A marked increase in the percentage degradation was observed in all pH ranges when the prepared catalysts were used. Cu/TiO_2/Bentonite, however, gave maximum efficiency in basic pH range.

4.3. Effect of concentration on degradation

The photocatalytic degradation efficiency of TiO_2/bentonite composite and Cu/TiO_2/bentonite composite were studied by using different amount of the catalyst. A major difference was found in the photocatalytic degradation efficiency of TiO_2/bentonite composite and Cu/TiO_2/bentonite composite. Cu/TiO_2/bentonite composite, however, showed better results as compared to TiO_2/bentonite composite.

The percentage efficiency of degradation was calculated and the results are shown below in Graph 3:

It can be seen that the percentage degradation efficiency of the Cu/TiO_2/bentonite is far superior to TiO_2/bentonite composite. The degradation decreased with the increasing dose of the catalyst indicating high sensitivity of a very small amount of the catalyst to catalyze the reaction. 0.02 g of the

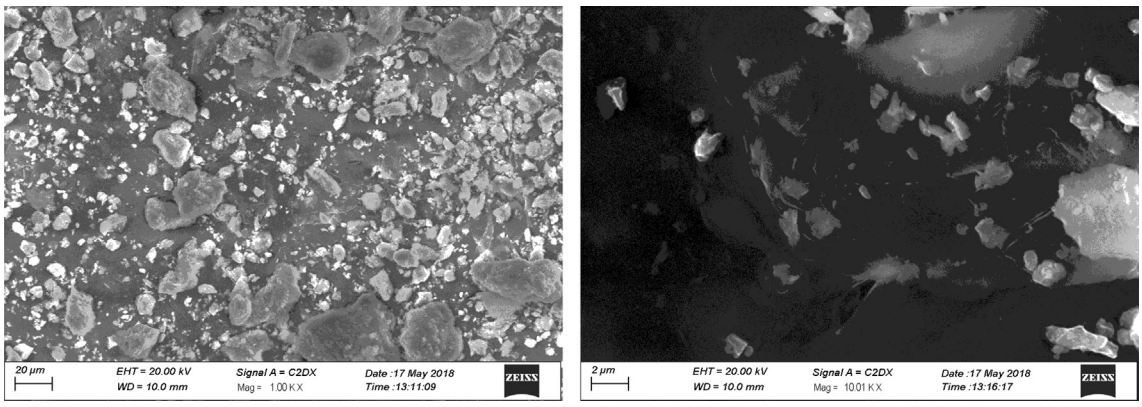

Fig. 3a TiO_2/bentonite composite.

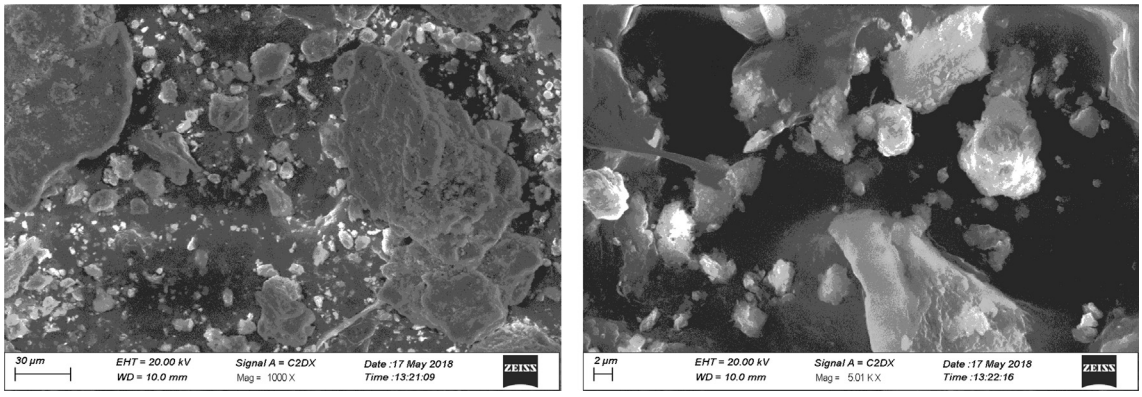

Fig. 3b Cu/TiO_2/bentonite composite.

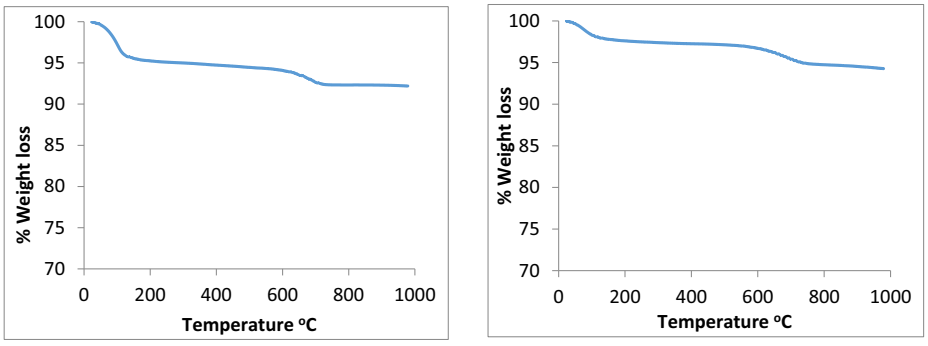

(a) TiO_2/bentonite Composite (b) Cu/TiO_2/bentonite Composite

Fig. 4 TGA of composites.

catalyst per 10 mL of 100 ppm deltamethrin is the optimum dose for maximum degradation. At higher concentration, catalysis aggregation takes place that lowers the surface area and activity of the catalyst.

4.4. Reaction statistics of photo-catalytic degradation of deltamethrin

The kinetics data of degradation of deltamethrin by TiO_2/bentonite composite and Cu/TiO_2/bentonite composite with contact time varying from 15 min to 120 min was studied. The data was suited for 1st order kinetic model (Pengyan et al., 2010). The data is shown in Graph 4 with TiO_2/bentonite composite.

In the presence of TiO_2/bentonite composite, the half-life of Deltamethrin in sunlight is 96 min. The rate constant was examined to be 7.2×10^{-3}. With Cu/TiO_2/bentonite composite the half-life of Deltamethrin reduced to 43 min with subsequent increase in rate constant, i.e. 1.21×10^{-2}. (See Graph 5)

It was observed that the half-life of insecticide was reduced in the presence of Cu/TiO_2/bentonite composite. The data of half-life displayed that a rapid degradation took place in the

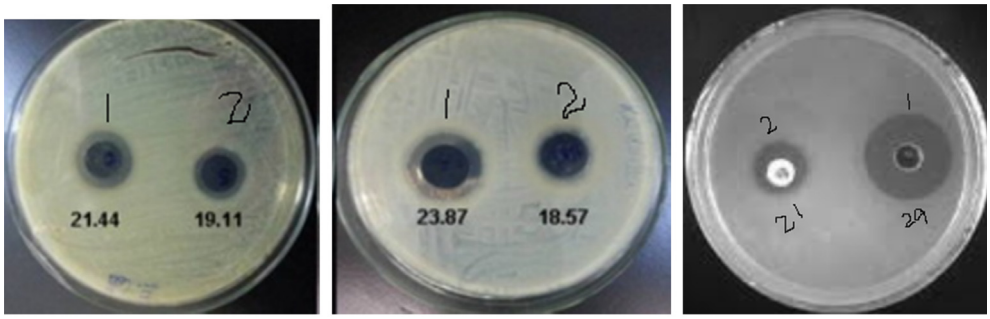

(a) (b) (c)

Fig. 5 Zone of inhibition measured (mm) for antibacterial activity of composite evaluated on (a) Escherichia. Coli (b) Staphylococcus aureus (c) Ciprofloxacin.

presence of Cu/TiO_2/bentonite composite in sunlight in minimum time.

4.5. Antibacterial tests

Comparative analysis of the antibacterial activity of TiO_2/bentonite composite and Cu/TiO_2/bentonite composite were tested against gram positive S. aureus bacterium and gram negative E. coli bacterium using the well diffusion method. Fig. represents the images of the antibacterial tests and the results are mentioned in Table 1. The result showed that Cu/TiO_2/bentonite composites possess good anti-bacterial activity i.e. 23.87 mm for S. aureus, 21.44 mm for E. Coli and 29 mm for Ciprofloxacin. There are few studies reporting the mechanism of the antibacterial property shown by the composites. It has been stated that the release of ions includes Ti^{+2}, Cu^{+}, Si^{+4}, Al^{+3} and Mg^{+} from the composite are accountable are accountable for the exhibited antibacterial property of the materials (Min et al., 2010). Also, small sized particles allow the enhanced dispersion and interaction with the bacteria which causes cellular inactivation and leads to the cell death (Pandiyarajan et al., 2013).

Bacterial cell walls are normally negatively charged due to the presence of anions in lipid bilayer. The cations released from the composite strongly binds with the anions that hinders the metabolism of cellular processes (Azam et al., 2012). This is the main reason for the antibacterial activity possessed by the composites (Sohrabnezhad et al., 2014).

5. Conclusion

In summary, TiO_2/bentonite and Cu/TiO_2/bentonite composites were synthesized. The composites were thermally stable up to 1000 °C. The prepared materials were used for the degradation of deltamethrin. Different parameters were studied for degradation process. It was observed that photo degradation of Deltamethrin is pH dependent and maximum removal occurs at pH 12. By increasing the catalyst concentration, percentage removal decreased indicating that a very small amount of the catalyst is required for the degradation. Degradation of the insecticide increased with an increase in time up to 120 min and maximum degradation of 87.01% in the case of TiO_2/bentonite composite and 97.48% in the presence of Cu/TiO_2/bentonite composite was observed. The photodegradation follows first order kinetics.

References

Barbosa, L.B., Marcal, L., Nassar, E.J., Calefi, P.S., Vicente, M.A., Trujillano, R., Rives, V., Gil, A., Korili, S.A., Ciuffi, K.J., de Faria, E.H., 2015. Kaolinite-titanium oxide composites prepared via sol-gel as heterogeneous photocatalysts for dye degradation. Catal. Today 246, 133.

Tamayo, L., Azocar, M., Kogan, M., Riveros, A., Paez, M., 2016. Copper-polymer composites: An excellent and cost-effective biocide for use on antibacterial surfaces. Mater. Sci. Eng. C 69, 1391.

Samavati, A., Ismail, A.F., 2017. Antibacterial properties of copper-substituted cobalt ferrite nanoparticles synthesized by co-precipitation method. Particuology 30, 158.

Radhakrishnan, A.A., Beena, B.B., 2014. Structural and Optical Absorption Analysis of CuO. Indian Journal of Advances in Chemical Science 2, 158.

Yu, K., Huang, L., Lou, L.L., 2015. Degradation of polycyclic aromatic hydrocarbons in crumb tyre rubber catalyzed by rutile TiO2 under irradiation. Environ technology 36, 1008.

Li, C.Q., Sun, Z.M., Xue, Y.L., Yao, G.Y., Zheng, S.L., 2016. A facile synthesis of g-C_3N_4/TiO_2 hybrid photocatalysts by sol-gel method and its enhanced photo degradation towards methylene blue under visible light. Adv. Powder. Technol 27, 330.

Katerina, D., Katerina, M., Jawslar, L., Pavline, P., Katerina, K.M., Lucie, N., Karel, F., 2014. Antibacterial activity of Kaolinita/nano

Table 1 Zone of inhibition measured (mm) for antibacterial activity.

Sr. #	Samples	S. aureus (mm)	E. coli (mm)	Ciprofloxacin (+ve control)
1	Cu/TiO_2/bentonite	23.87	21.44	29
2	TiO_2/bentonite	18.57	19.11	21

TiO_2 composite in relation to irradiation time. J. Photochem. Photobiol., B 135, 17.
Daniel, L.M., Frost, R.L., Zhu, H.Y., 2007. Synthesis and characterization of clay supported titania photocatalysts. J. Colloid Interface Sci. 316, 72.
Kim, J.S., Sung, H.J., Kim, B.J., 2015. Photocatalytic characteristics for the nanocrystalline TiO_2 on the Ag-doped $CaAl_2O_4$:(Eu, Nd) phosphor. Appl. Surf. Sci. 334, 151.
Islam, S.Z., Reed, A., Kim, D.Y., Rankin, S.E., 2016. N_2/Ar Plasma-induced doping of ordered mesoporous TiO_2 thin films for visible light active photocatalysis. Microporous Mesoporous Mater 220, 120.
Zoltan, T., Rosales, M.C., Yadorola, C., 2016. Reactive oxygen species quantification and their correlation with the photocatalytic activity of TiO_2 (anatase and rutile) sensitized with asymmetric porphyrins. J. Environ. Chem. Eng 4, 3967.
Daghrir, R., Drogui, P., Robert, D., 2013. Modified TiO_2 for environmental photocatalytic applications. Ind. Eng. Chem. Res 52, 3581.
Valisaki, E., Georgaki, I., Vernardore, D., Vamvakaki, M., Katsarkis, N., 2015. Ag-loaded TiO_2/reduced graphene oxide composite for enhanced visible light photocatalytic activity. Appl. Surf. Sci. 353, 865.
Qi, L., Yu, J., Lix, G., Wong, P.K., 2014. Synthesis and photocatalytic activity of plasmonic AgCl composite immobilized on titanate nanowire. Catal. Today 224, 193.
J. Fu, S. CaO, J. Yu., dual Z-scheme charge transfer in TiO2-Ag-Cu2O composite for enhanced photocatalytic hydrogen generation, J. Materiomics 1, 124 (2015).
Jesus, H.V., Sandrine, C., Antonieta, M.G., Felipe, R.C., Abdelhadi, K., 2017. Effects of metal dopping (Cu, Ag, Eu) on the electronic and optical behavior of nanostructured TiO_2. J. Alloy Compod. 710, 355.
Chien-Wei, C., Chechia, H., 2020. Graphene oxide-derived carbon-doped SrTiO3 for highly efficient photocatalytic degradation of organic pollutants under visible light irradiation. Chem. Eng. J. 383, 123116.
Hsiao-Han, W., Chien-Wei, C., Daling, L., Kazuhiko, M., Chechia, H., 2019. Synergistic Effect of Hydrochloric Acid and Phytic Acid Doping on Polyaniline-Coupled g-C3N4 Nanosheets for Photocatalytic Cr(VI) Reduction and Dye Degradation. ACS Appl. Mater. Interf. 11, 35702.
Amit, M., Akansha, M., Manisha, S., Soumen, B., 2017. Impact of Ag nanoparticles on photomineralization of chlorobenzene by TiO_2/bentonite composite, *Journal of Environmental*. Chem. Eng. 5, 644.
Rashid, S.M., Verbeeka, C.J.R., Mark, L.C., 2016. Settling of Bentonite Particles in Gelatin Solutions for Stickwater Treatment. Procedia Engineering 6, 570.
Szczepanik, B., 2017. Photocatalytic degradation of organic contaminants over clay-TiO2 nanocomposites: A review. Appl. Clay Sci. 171, 227.
Papoulis, D., Somalakidi, K., Todorova, N., Trapalis, C., Panagiotaras, D., Sygkridou, D., Stathatos, E., Gianni, F., Mavrikos, A., Komarneni, 2019. Sepiolite/TiO2 and metal ion modified sepiolite/TiO2 nanocomposites: synthesis, characterization and photocatalytic activity in abatement of NOx gases. Appl. Clay Sci. 179.
Seftel, E.M., Niarchos, M., Mitropoulos, Ch, Mertens, M., Vansant, E.F., Cool, P., 2015. Photocatalytic removal of phenol and methylene-blue in aqueous media using TiO2@LDH clay nanocomposites. Catal. Today 252, 120.
Zhirong, I., Uddin, M.A., Zhanxue, S., 2011. FTIR and Xrd Analysis of natural Na-bentonite and Cu(II) loaded Na-bentinite,. Spectrochim. Acta Part A Mol. Biomol. Spectroscopy 79, 1013.
Erin, E., Tabak, A., Eren, B., 2010. Performance of magnesium oxide coated bentonite in removal process of copper ions from aqueous solution. Desalination 257, 163.
Desai, V.S., Kowshik, M., 2009. Antimicrobial activity of titanium dioxide nanoparticles synthesized by sol-gel technique. Res. J. Microbiol 4, 97.
Andrea Leon, L., Patricia Reuquen, R., Carolina, G., Rodrigo, S., Patricio, V., Paula, Z., Pedro, A., 2017. FTIR and Raman Characterization of TiO_2 Nanoparticles Coated with Polyethylene Glycol as Carrier for 2-Methoxyestradiol. Applied Sciences 7, 49.
Nien, Y.T., Liao, Y.H., Liao, P.C., 2011. Antibacterial activity of poloxamer modified montmorillonite clay against E. Coli. Mater. Lett 65, 3092.
Deak, A.G., Janovak, L.S., Tallosy, S.P.T., Bito, T.S., Sebok, D.N., Buzas, N., Palinko, I.N., Dekany, I., 2015. Spherical LDH-Ag-montmorillonite heterocoagulated system with a pH-dependent sol-gel structure for controlled accessibility of AgNPs immobilized on the clay lamellae. Langmuir 31, 2019.
Rosario, J.A.D., Moura, G.B., Gusatti, M., Riella, H.G., 2009. Synthesis of silver treated bentonite: evaluation of its antibacterial properties. Chem. Eng. 17.
Pengyan, L., Yujie, L., Qingxue, L., Jinwei, L., 2010. Photodegradation mechanism of deltamethrin and fenvalerate. J. Environ. Sci. 22, 1123.
Min, S.H., Yang, J.H., Kim, J.Y., Kwon, Y.U., 2010. Development of white antibacterial pigment based on silver chloride manoparticles and mesoporous silica and its polymer composite. Micropor. Mesopor. Mater. 128, 19.
Pandiyarajan, T., Udayabhaskar, R., Vignesh, S., James, R.A., Karthikeyan, B., 2013. Synthesis and concentration dependent antibacterial activities of CuO nanoflakes. Mater. Sci. Eng C 33, 2020.
Azam, A., Ahmed, A.S., Oves, M., Khan, M., Memic, A., 2012. Size dependent antimicrobial properties of CuO nanoparticles against gram positive and gram negative bacterial strains. Int. J. Nanomed. 7, 3527.
Sohrabnezhad, S., Moghaddam, M.M., Salavatiyan, T., 2014. Synthesis and characterization of CuO-montmorillonite composite by thermal decomposition method and antibacterial activity of composite. Spectrochime Acta Part A Mol. Biomol. Spectroscopy 125, 73.